

## Ionic liquid intercalated $V_2O_5$ nanorods: synthesis and characterization

K MANJUNATH<sup>1</sup>, V D'SOUZA<sup>2</sup>, J DUPONT<sup>2</sup>, T RAMAKRISHNAPPA<sup>1</sup> and G NAGARAJU<sup>1,3,\*</sup>

<sup>1</sup>Centre for Nano and Materials Science, Jain University, Jakkasandra (P), Kanakapura, India

<sup>2</sup>Laboratory of Molecular Catalysis, Institute of Chemistry, UFRGS, Porto Alegre, Brazil RS

<sup>3</sup>Department of Chemistry, Siddaganga Institute of Technology, Tumkur, India

MS received 16 January 2015; accepted 7 May 2015

**Abstract.** In this work, ionic liquid (IL) intercalated  $V_2O_5$  (IL- $V_2O_5$ ) nanorods have been synthesized through the IL-assisted hydrothermal method using imidazolium-based functionalized IL at 130°C for 3 days. The structure and morphology of the obtained product was characterized using various techniques. X-ray diffraction pattern reveals the intercalation of IL at  $2\theta = 7^\circ$  in orthorhombic  $V_2O_5$ . The Fourier transform infrared spectrum shows a band at  $1044\text{ cm}^{-1}$ , which could be assigned to stretching vibration of terminal vanadyl (V=O), sensitive to cation intercalation between vanadium oxide layers. UV-vis absorption spectrum of IL- $V_2O_5$  nanorods and calcined  $V_2O_5$  nanoparticles show a maximum absorbance at 402 and 420 nm, respectively. The morphology of the product was investigated by scanning electron microscopy and transition electron microscopy (TEM). TEM analysis reveals the nanorods with thickness of 30–50 nm.

**Keywords.** Vanadium pentoxide; nanorods; ionic liquid; hydrothermal.

### 1. Introduction

There has been an explosive growth of nanoscience and nanotechnology in the last two decades primarily because of the availability of new methods of synthesizing nanomaterials, as well as tools for the characterization and manipulation.<sup>1</sup> In recent times, it has been demonstrated that the synthesis of several new geometrical configurations with controlled morphology are of special interest owing to their unique periodic and elastic properties, resulting in structural flexibility that provides additional opportunities for nanoengineering. In recent days, the synthesis and characterization of 1-D nanostructured transition metal oxides have received considerable attention due to their novel application,<sup>2–4</sup> including cathode materials for lithium ion battery, catalyst for photocatalytic degradation, microelectronic circuits, sensors, piezoelectric devices, fuel cells and as coatings for the passivation of surfaces against corrosion. Among the transition metal oxides, vanadium oxides and their derived nonstructural compounds particularly show rich chemistry. Vanadium pentoxide ( $V_2O_5$ ) is a semiconductor with an optical bandgap of 2.38 eV at room temperature and is an important transition metal oxide. This class of materials exhibits a wide range of electronic and ionic properties.<sup>5,6</sup> This compound is widely studied and is a promising

material, both in the pure form and in the composite form with macromolecular moieties.  $V_2O_5$  possess tunable oxidation states<sup>7</sup> and flexible coordination environment.<sup>8</sup> It finds a variety of applications in electronic switching devices<sup>9,10</sup> and electrode materials for lithium battery. Vanadium oxides exhibit a layered structure and are well known for their intercalation properties. A large variety of vanadium oxide-based compounds have been described, in which cations, transition metal complexes, organic molecules and even polymers have been intercalated. Among them, cation intercalated xerogels  $M_xV_2O_5 \cdot mH_2O$  ( $M = Li^+, Na^+, NH_4^+$ , organic cations like imidazolium ions, etc.) gained more interest. Nagaraju and Chandrappa<sup>11</sup> have synthesized  $Na_{0.28}V_2O_5$  nanobelts via intercalation of sodium ions by the hydrothermal method. Chandrappa *et al*<sup>2</sup> have synthesized  $(NH_4)_{0.5}V_2O_5 \cdot mH_2O$  nanobelts, triangles, rings via intercalation of ammonium ions through the hydrothermal method. Wang *et al*<sup>12</sup> have synthesized  $(NH_4)_2V_6O_{16} \cdot 1.5H_2O$  nanowires,  $(NH_4)_6V_{10}O_{28} \cdot 6H_2O$  nanobundles,  $NH_4V_4O_{10}$  nanobelts, via intercalation of different amounts of ammonium ions using the hydrothermal method. Zoubi *et al*<sup>13</sup> have synthesized  $V_2O_5$  nanoparticles via intercalation of different ionic liquids (ILs) as well as organic solvents using the sol-gel method. Various morphologies of vanadium oxide and its derived compounds such as nanotubes, nanowires, nanofibres, nanobelts, nanorods and mesoporous structures in micro/nanostructures have so far been successfully synthesized by using a variety of synthetic routes such as the

\*Author for correspondence (nagarajugn@rediffmail.com)

hydrothermal, solvothermal, ionothermal, combustion method and so on.<sup>14–21</sup> Among them the hydrothermal method has several advantages in terms of synthesis control: the control of parameters such as reaction temperature, pH and solvent concentration, as well as the addition of templates or additives, making it possible to obtain with different morphologies and structures in a simple way.<sup>22</sup> During the hydrothermal process, supercritical water plays the role of reducing agent and also behaves as green solvent.<sup>23</sup>

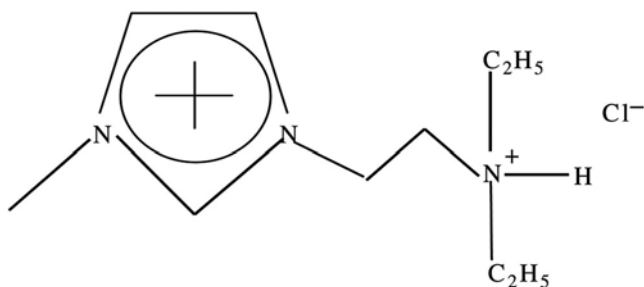
In recent years, ILs have attracted an increasing interest for its preparation of inorganic metal oxides. The obvious advantages of ILs over conventional organic solvents and electrolytes are their non-flammability, non-volatility, high thermal stability and wide liquid range stability and coordination ability. These ILs can be fine tuned by altering the cation or anion to specific applications. Hence ILs have been referred to as ‘designer solvents’ or ‘tailor-made solvents’.<sup>24–26</sup> In this work, we report the preparation of IL intercalated  $V_2O_5$  (IL- $V_2O_5$ ) nanorods through the one pot hydrothermal route at 130°C for 2 days.

## 2. Experimental

Briefly, 0.16 g  $V_2O_5$  was added to the 2 ml hydrogen peroxide ( $H_2O_2$ ). Brisk effervescence was observed and the mixture turned black. In total, 40 ml water was added followed by the addition of 0.5 g of IL [N,N-diethyl, ethyl amine methyl imidazolium hydrogen chloride (DEEAMI)]. The mixture was stirred well to obtain homogeneous solution. After stirring, the mixture was transferred to Teflon tube, subjected to the hydrothermal treatment at 130°C for 2 days. After the hydrothermal treatment, autoclaves were cooled to room temperature. The obtained product was centrifuged, washed with distilled water and ethanol several times to the remove impurities. It was then dried in an oven at 80°C overnight and calcined at 400°C for 3 h.

### 2.1 Preparation of DEEAMI

IL was prepared using our earlier report.<sup>27</sup> Briefly, 232.4 mmol of 1-methyl imidazole and 232.4 mmol of



**Scheme 1.** Structure of N,N-diethyl, ethyl amine methyl imidazolium hydrogen chloride.

2-chloro-N,N-diethyl amine hydrochloride were mixed in acetonitrile (200 ml) and subjected to reflux condition. After 4–5 days of reaction, a white solid was separated by filtration and washed with 1 : 1 mixture of diethyl ether and acetonitrile. The resultant white solid was dried under reduced pressure at 100°C for 1 day.

### 2.2 Characterization

Powder X-ray diffraction (XRD) data were recorded on Philips X'pert PRO PANalytical X-ray diffractometer with graphite monochromatized  $CuK\alpha$  (1.5418 Å) radiation. The Fourier transform infrared (FTIR) spectra of the samples were collected using Bruker Alpha-P spectrometer. Raman spectra were recorded (LabRAM HR, Horiba Jobin Yvon, France) using a 514.5 nm, air-cooled  $Ar^+$  laser with 50× objective and with laser intensity. The absorption spectra of the samples were measured on a Shimadzu UV-1800 UV–visible spectrophotometer. Thermal analysis data were obtained using thermogravimetric analyser 2950 (DuPont instruments). The morphology of the products were examined using Carl Zeiss Ultra 55 scanning electron microscopy (SEM) and JEOL JEM 1200 Ex. transmission electron microscopy (TEM).

## 3. Results and discussion

Figure 1 shows XRD patterns of IL- $V_2O_5$  nanorods and  $V_2O_5$  nanoparticles, respectively, synthesized at 130°C for 2 days using DEEAMI. In figure 1a, the intensities of the peaks are reduced due to intercalation of IL at  $2\theta = 7^\circ$ . We investigated the effect of calcination on the crystallization and morphology of the IL- $V_2O_5$  nanorods. After calcination at 400°C for 3 h, IL- $V_2O_5$  leads to pure crystalline  $V_2O_5$ . All the XRD peaks shown in figure 1b

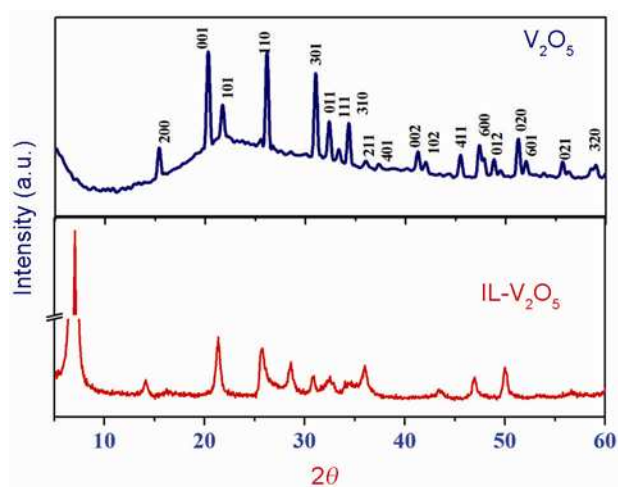


**Figure 1.** XRD patterns of (a) IL- $V_2O_5$  and (b) calcined  $V_2O_5$ .

could be attributed to the orthorhombic shcherbaniite V<sub>2</sub>O<sub>5</sub> phase (JCPDS no. 03-207 with  $a = 11.48 \text{ \AA}$ ,  $b = 4.36 \text{ \AA}$ ,  $c = 3.55 \text{ \AA}$ ), indicating that all intercalated molecules were driven out leading to V<sub>2</sub>O<sub>5</sub>.

Figure 2 shows the FTIR spectrum of IL-V<sub>2</sub>O<sub>5</sub> nanorods and calcined V<sub>2</sub>O<sub>5</sub> nanoparticles. The absorption band at 708 cm<sup>-1</sup> is assigned to V–O–V asymmetric stretching vibration. The band centred at 977 cm<sup>-1</sup> is assigned to V=O stretching vibration, which is sensitive to intercalation and suggests that IL is intercalated between vanadium oxide layers. The splitting of 977 cm<sup>-1</sup> band into two absorption peaks (963 and 993 cm<sup>-1</sup>) as compared to standard V<sub>2</sub>O<sub>5</sub> (~1020 cm<sup>-1</sup>) arises from the formation of two inequivalent V=O groups. The bands at 963 and 993 cm<sup>-1</sup>, respectively, are assigned to the V=O stretching of disorted octahedral and disorted square pyramids. The band at 1044 cm<sup>-1</sup> is a characteristic peak corresponding to vibration of terminal vanadyl V=O. The bands at 1459 and 1561 cm<sup>-1</sup> are assigned to C=C stretching modes. The band at 1628 cm<sup>-1</sup> is due to water molecule. The characteristic bands at 3097 and 3143 cm<sup>-1</sup> are due to imidazolium ring. The peaks corresponding to imidazole ring disappear due to calcination leaving behind the unchanged V<sub>2</sub>O<sub>5</sub>.

Figure 3 shows the Raman spectra of IL-V<sub>2</sub>O<sub>5</sub> nanorods and calcined V<sub>2</sub>O<sub>5</sub> nanoparticles, respectively. In case of IL-V<sub>2</sub>O<sub>5</sub> nanorods the known V–O–V modes were observed at 407, 520 cm<sup>-1</sup>, while other bands below 400 cm<sup>-1</sup> can be assigned to V–O and V–O–V bending modes. The band at 990 cm<sup>-1</sup> is due to V=O stretching of disorted octahedral and square pyramids, while the band at 692 cm<sup>-1</sup> is due to coordination of vanadium atoms with the three oxygen atoms<sup>28</sup> as shown in figure 3a. But in figure 3b, the peaks at 826, 876 cm<sup>-1</sup> are disappeared after calcination at 400°C for 3 h. This proves that the IL indeed had remained intercalated, which gets eliminated on calcination.

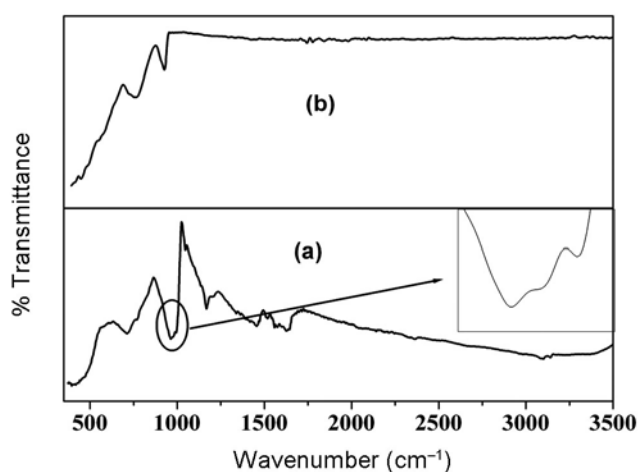


**Figure 2.** FTIR spectrum of (a) IL-V<sub>2</sub>O<sub>5</sub> and (b) calcined V<sub>2</sub>O<sub>5</sub>.

UV–vis spectra of IL-V<sub>2</sub>O<sub>5</sub> nanorods and calcined V<sub>2</sub>O<sub>5</sub> nanoparticles are shown in figure 4. From figure 4a it can be observed that the absorption peak at 268 nm is due to the presence of IL, which dominates the spectrum, even after extensive washing<sup>29</sup> and at 402 nm ( $E_g = 3.09 \text{ eV}$ ) is due to V<sub>2</sub>O<sub>5</sub>. However in figure 4b a single absorption peak around 420 nm ( $E_g = 2.9 \text{ eV}$ ) and the peak at 268 nm is disappeared due to calcination at 400°C for 3 h. The absorption band at 420 nm ( $E_g = 2.09 \text{ eV}$ ) was red shifted compared to IL-V<sub>2</sub>O<sub>5</sub> due to agglomeration of V<sub>2</sub>O<sub>5</sub> nanoparticles.

Figure 5 shows the thermogravimetric analysis of IL-V<sub>2</sub>O<sub>5</sub> nanorods. It clearly shows the decrease in weight up to 400°C. Weight loss up to 100°C is due to the

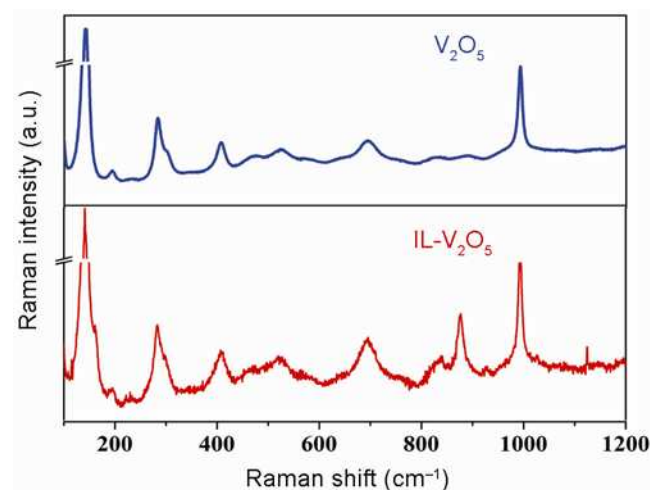


**Figure 3.** Raman spectrum of (a) IL-V<sub>2</sub>O<sub>5</sub> and (b) calcined V<sub>2</sub>O<sub>5</sub>.

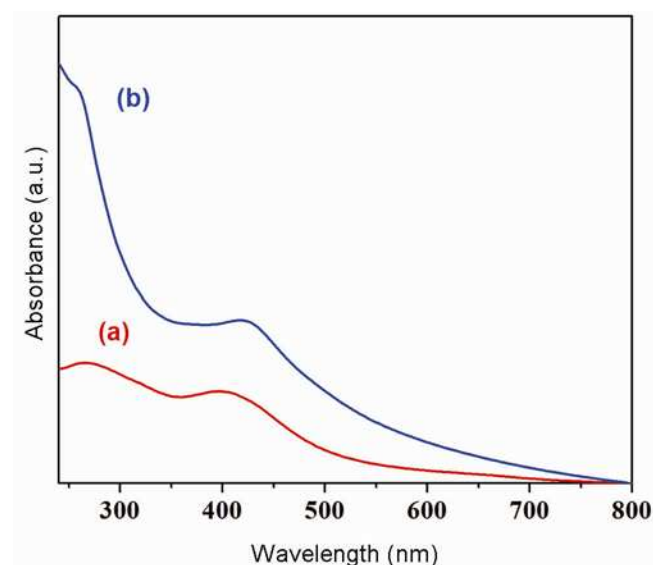


**Figure 4.** UV–vis spectrum of (a) IL-V<sub>2</sub>O<sub>5</sub> and (b) calcined V<sub>2</sub>O<sub>5</sub>.

removal/desorption of water and alcohol. Further decrease in weight loss is due to the presence of IL. After 400°C there is no weight loss observed. It clearly indicates that 400°C is sufficient to remove intercalated IL from  $V_2O_5$ . Thermogravimetric analysis clearly shows that it contains about 6% of IL and the product is stable up to 700°C.

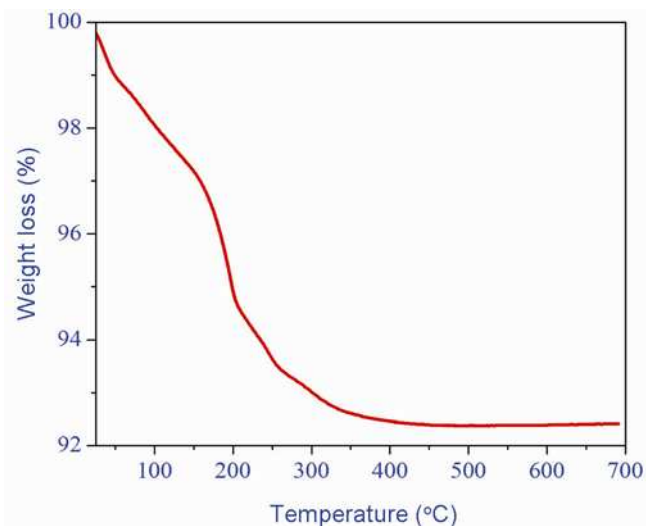


Figure 5. Thermogravimetric analysis of IL- $V_2O_5$ .

The morphology of the product was examined by SEM. Figure 6 shows SEM images of IL- $V_2O_5$  and calcined  $V_2O_5$  nanoparticles. After 2 days (figure 6a), the product exhibits large-scale rod-like morphology with blunt ends and arranged like a stacking to each other. The thicknesses of the nanorods are in the range of 90–120 nm with typical lengths up to several tens of micrometres. The effect of calcination on the morphology of IL- $V_2O_5$  nanorods in addition to structure was investigated. It clearly shows that after calcination at 400°C for 3 h, pure  $V_2O_5$  nanoparticles are obtained.

The morphology of the product was further examined by TEM. Figure 7a and b shows the TEM images of IL- $V_2O_5$  nanorods. The product exhibits rod-like morphology and confirmed that the width and thickness of the nanorods are in the range of 30–50 nm, respectively.

#### 4. Conclusion

Orthorhombic  $V_2O_5$  nanorods were successfully synthesized by a simple low-temperature hydrothermal method at 130°C for 3 days. XRD pattern reveals that the as-prepared product is IL intercalated orthorhombic  $V_2O_5$ . The FTIR spectrum shows a band at  $1044\text{ cm}^{-1}$ , which could be assigned to stretching vibration of terminal

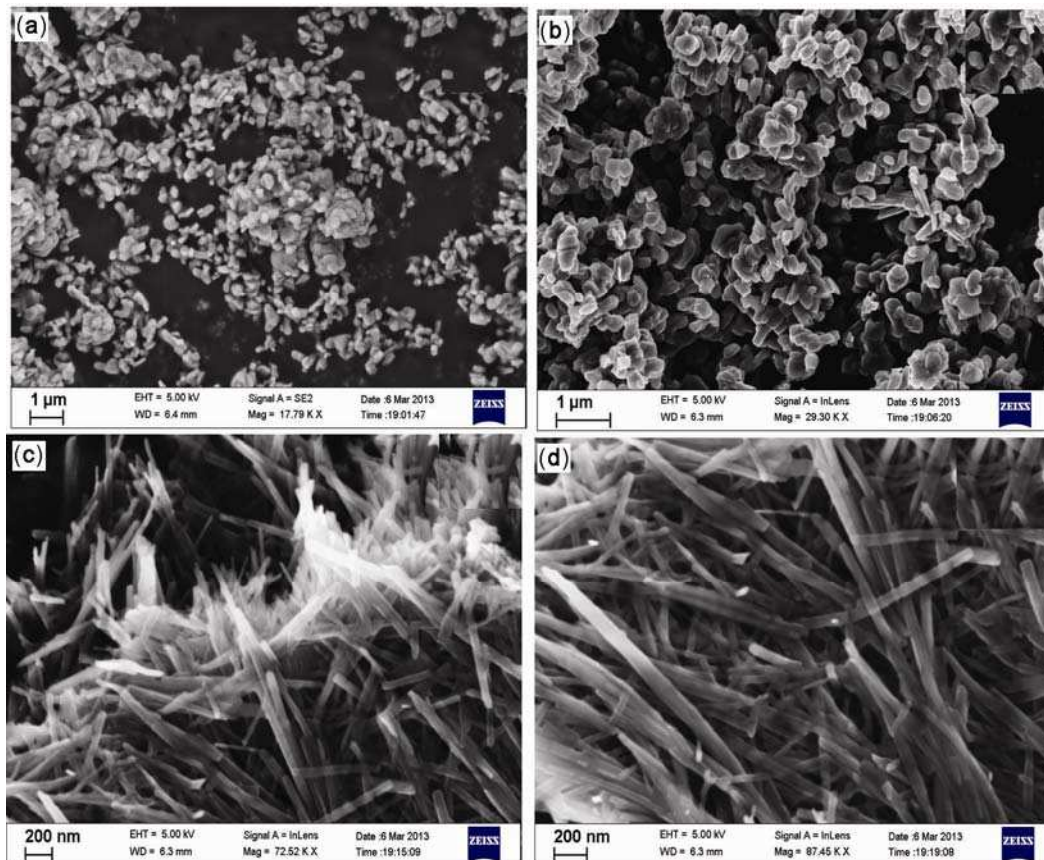
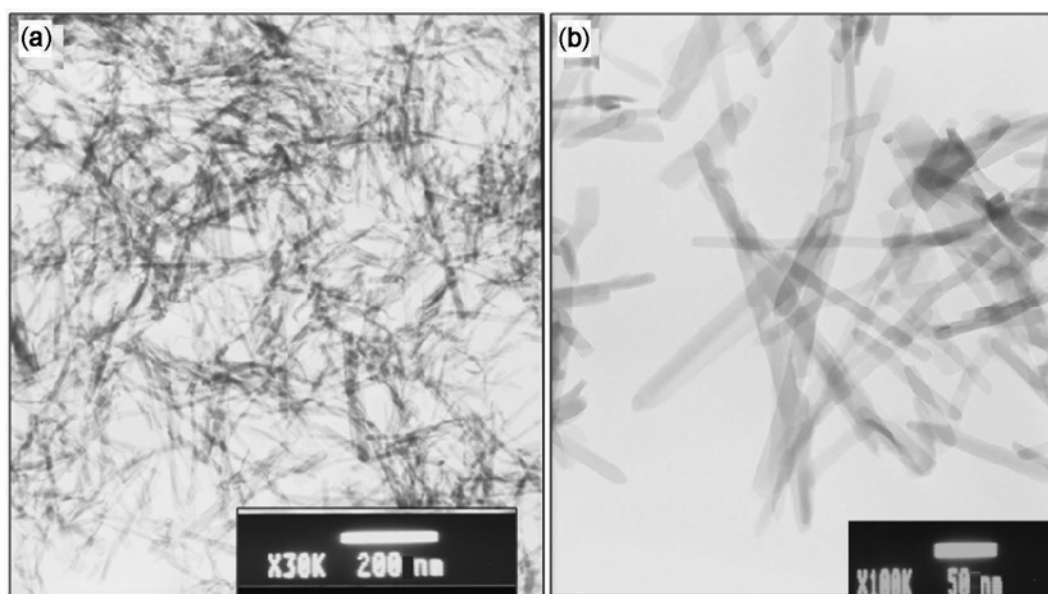


Figure 6. SEM images of (a, b) IL- $V_2O_5$  and (c, d) calcined  $V_2O_5$ .



**Figure 7.** TEM images of IL-V<sub>2</sub>O<sub>5</sub>.

vanadyl (V=O), sensitive to cation intercalation between vanadium oxide layers. UV-vis absorption spectrum shows the presence of IL in the as-prepared V<sub>2</sub>O<sub>5</sub> nanorods. Effect of calcination clearly indicates the increase of crystallite size, which is observed by red shift in UV-vis study. TEM images show that the thickness of the nanorods are of 30–50 nm.

#### Acknowledgement

Mr K Manjunath acknowledges Jain University for providing financial support for this research work. Dr G Nagaraju thanks Siddaganga Institute of Technology for constant support and encouragement.

#### References

- Schlessler R, Dalmau R, Zhuang D, Collazo R and Sitar Z 2005 *J. Cryst. Growth* **281** 75
- Chandrappa G T, Chithaiah P, Ashoka S and Livage J 2011 *Inorg. Chem.* **50** 7421
- Duan X, Niu C, Sahi V, Chen J, Parce J, Empedocles S and Goldman J 2003 *Nature* **425** 274
- Zhong Z, Wang D, Cui Y, Bockrath M and Lieber C M 2003 *Science* **302** 1377
- Livage J 1991 *Chem. Mater.* **3** 578
- Moshfegh A Z and Ignatiev A 1991 *Thin Solid Films* **198** 251
- Sphar M E, Stoschitzki B P, Nesper R, Hass O and Novak P 1999 *J. Electrochem. Soc.* **146** 2780
- Cao J, Musfeldt J L, Mazumdar S, Chernova N A and Whittingham M S 2007 *Nano Lett.* **7** 2351
- Barboux P, Baffier N, Morineau R, Livage J, Goodenough J B, Jensen J and Poiter A 1985 *Solid state protonic conductors III* (Paris: Odense University Press) p 173
- Livage J 1984 *Mater. Res. Soc. Symp. Proc.* **32** 125
- Nagaraju G and Chandrappa G T 2012 *Mater. Res. Bull.* **47** 3216
- Wang N, Chen W and Mail D Y 2008 *J. Solid State Chem.* **181** 652
- Zoubi M A, Hala K F and Frank Endres 2009 *J. Mater. Sci.* **44** 1363
- Durupthy O, Steunou N, Coradin T, Maquet J, Bonhomme C and Livage J 2005 *J. Mater. Chem.* **15** 1090
- Han W, Fan S, Li Q and Hu Y 1997 *Science* **277** 1287
- Li Y D, Liao H W, Ding Y, Fan Y, Zhang Y and Qian Y T 1999 *Inorg. Chem.* 381
- Pinna N, Wild U, Urban J and Schlogl R 2003 *Adv. Mater.* **15** 329
- Ribeiro W A C, Leite E R and Mastelaro V R 2009 *Cryst. Growth Des.* **9** 3626
- Rothschild A, Sloan J and Tenne R 2000 *J. Am. Chem. Soc.* **122** 5169
- Wang Y and Cao G 2006 *Chem. Mater.* **18** 2787
- Zhou F, Zhao X, Yuan C and Li L 2008 *Cryst. Growth Des.* **8** 7
- Nagaraju G 2012 *Z. Anorg. Allg. Chem.* **638** 2286
- Zhou Y, Bao Q, Tang L L, Zhong Y and Loh K P 2009 *Chem. Mater.* **2** 2950
- Dupont J, De Souza R F and Suarez P A Z 2002 *Chem. Rev.* **102** 3667
- Dupont J and Jackson D S 2010 *Chem. Soc. Rev.* **39** 1780
- Hu H, Yang H, Huang P, Cui D, Peng Y, Zhang J, Lu F, Lian J and Shi D 2010 *Chem. Commun.* **46** 3866
- Cassol C C, Ebeling G, Ferrera B and Dupont J 2006 *Adv. Synth. Catal.* **348** 243
- Israel E and Waches 2001 *Raman spectroscopy of catalysis, Hand book of Raman spectroscopy* (Pennsylvania: CRC Press, Lehigh University) p 799
- Nagaraju G, Ebeling G, Goncalves R V, Teixeira S R, Weibel D E and Dupont J 2013 *J. Mol. Catal. A – Chem.* **378** 213